Electronic Supplementary Material (ESI) for RSC Advances.
This journal is © The Royal Society of Chemistry 2017

Supporting Information

Upgrading of palmitic acid over MOF catalysts in supercritical fluid of n-hexane

Xiao Fang[a], Yanchun Shi[a], Kejing Wu[a], Junmei Liang[a], Yulong Wu[a,b*], Mingde Yang[a]

a: Institute of Nuclear and New Energy Technology, Tsinghua University, Beijing 100084, PR China

b: Beijing Engineering Research Center for Biofuels, Beijing 100084, China

*Corresponding author: Prof. Dr. Yulong Wu

Address: Institute of Nuclear and New Energy Technology, Tsinghua University, Beijing 100084, PR China

Tel: +86 010-89796163; Fax: +86 10-69771464

E-mail: wylong@tsinghua.edu.cn (Y. L. Wu)

MOF-5 hollow nanospheres

In a typical procedure, $Zn(NO_3)_2 \cdot 6H_2O$ 11.6 mg, H_2BDC 2.4 mg, and PVP (MW= 30000, 150 mg) were dissolved in DMF-ethanol mixture (6.4 mL, v/v = 5:3) under magnetic stirring for 10 minutes at room temperature. The resulting homogeneous solution was transferred to a 12 mL Teflon-lined stainless-steel autoclave. The sealed vessel was then heated at 150 ^oC for 12 h before it was cooled to room temperature. The products were separated via centrifugation at 11000 rpm for 15 minutes and further purified with DMF and ethanol for several times. [1]

PTA@MOF-5 hollow nanospheres

11.6 mg $Zn(NO_3)_2 \cdot H_2O$, 2.4 mg H_2BDC, 150 mg PVP and 2.4 mg PTA were dissolved in 6.4 mL DMF-ethanol mixture (v/v = 5:3) under magnetic stirring for 10 minutes at room temperature. The resulting homogeneous solution was transferred to a 12 mL Teflon-lined stainless-steel autoclave. After heating the sealed vessel at 150 ^oC for 12 h it was cooled to room temperature. The products were separated via centrifugation at 11000 rpm for 15 min and further purified with DMF and ethanol for several times.

Preparation of Fe^{III}-MOF-5 hollow octahedral nanostructures.

In a typical procedure, $Fe(acac)_3$, 60 mg, $Zn(NO_3)_2 \cdot 6H_2O$ 46.4 mg, H_2BDC 9.6 mg, and PVP (M_W= 30000, 200 mg) were dissolved in DMF-ethanol mixture (25.6 mL, v/v = 5:3) under magnetic stirring for 10 minutes at room temperature. The resulting

homogeneous solution was transferred to a 40 mL Teflon-lined stainless-steel autoclave. The sealed vessel was then heated at 100 °C for 6 h before it was cooled to room temperature. The products were separated via centrifugation at 11000 rpm for 15 min and further purified with DMF and ethanol for several times. [1]

Synthesis of PdCu dendrites.

In a typical synthesis, PdCu dendrites were synthesized according to the previous report [1]. Briefly, $Pd(acac)_2$ (7.6 mg), $Cu(acac)_2$ (6.5 mg), and PVP (M_W = 30000, 50 mg) were were dissolved in DMF (4 mL) with stirred for 10 min at room temperature and heated to 150 °C for 4 h in a 12 mL Teflon-lined stainless-steel autoclave. The resulting products were separated via centrifugation at 11000 rpm for 15 minutes and further purified with ethanol for several times.

Synthesis of Pd NPs.

Pd NPs were synthesized using the same procedure as PdCu alloy NPs but without the addition of $Cu(acac)_2$ in the reaction solution. [1]

Synthesis of Au NPs.

Briefly, PVP (M_W= 30000, 50 mg), and $H_2C_2O_4$ (0.5 mmol, 63 mg) were dissolved in formamide (5 mL) and heated to 120 °C, and $HAuCl_4 \cdot 4H_2O$ aqueous solution (0.25mL, 0.2 M) was injected and the solution was maintained at 120 °C for 10 min. The products were separated via centrifugation at 10000 rpm for 5 minutes and

further purified with ethanol for several times. [2]

General nanoparticle encapsulation procedure.

For all nanoparticles ethanol was used as solvent. Typically, a 2 mL nanoparticles solution of desired concentration and PVP (M_W = 30000, 200 mg) were mixed with DMF-ethanol mixture (23.6 mL, v/v =5:3) under magnetic stirring for 10 min at room temperature. Then, $Fe(acac)_3$ 60mg, $Zn(NO_3)_2 \cdot 6H_2O$ 46.4 mg, H_2BDC 9.6 mg were added to the above solution under magnetic stirring for another 10 minutes. The resulting solution was transferred to a 40 mL Teflon-lined stainless-steel autoclave. The sealed vessel was then heated at 100 ^oC for 6 h before it was cooled to room temperature. The products were separatedvia centrifugation at 11000 rpm for 15 minutes and further purified with DMF and ethanol for several times. [1]

Characterization

Powder X-ray diffraction (PXRD) patterns of the samples were recorded on a Bruker D8-advance X-ray powder diffractometer operated at 40 kV voltage and 40 mA current with CuKα radiation (λ=1.5406 Å). Transmission electron microscopy (TEM) was performed on a JEM 2100 LaB6 TEM (JEOL). X-ray photoelectron spectroscopy (XPS) was performed on scanning X-ray microprobe (Quantera SXM, ULVAC-PHI. INC) operated at 250 kV, 55 eV with monochromated Al Kα radiation. Binding energies were corrected by reference to the C 1s peak at 284.8 eV. Fourier-transformed infrared resonance (FT-IR) spectra were obtained in transmission

mode on a Perkin-Elmer Spectrum 100 spectrometer (Waltham, MA, USA). Thermogravimetric (TG) analysis was carried out at a constant heating rate of 10 ^{o}C min^{-1} from room temperature to 700 ^{o}C in N_2 atmosphere, using a TA-50 thermal analyzer. Elemental analysis of Pd, Cu and W in the solid samples was determined by inductively coupled plasma atomic emission spectrometry (ICP-AES, IRIS Intrepid II XSP, ThermoFisher). The surface area was calculated by the Brunauer-Emmett-Teller (BET) method, and the pore size distribution was calculated by the Barrett - Joyner - Halenda (BJH) method.

Figure captions:

Fig. S1 TEM image of MOF-5.

Fig. S2 TEM image of PTA@MOF-5.

Fig. S3 TEM image of FeIII-MOF-5.

Fig. S4 TEM image of PdCu@FeIII-MOF-5.

Fig. S5 TEM image of Pd NPs@FeIII-MOF-5.

Fig. S6 TEM image of Au NPs@FeIII-MOF-5.

Fig. S7 TEM image of PdCu dendrites.

Fig. S8 TEM image of Pd NPs.

Fig. S9 TEM image of Au NPs.

Fig. S10 XRD analysis of FeIII-MOF-5.

Fig. S11 XPS spectra of PTA@FeIII-MOF-5 hollow octahedral nanostructures: (a) The survey spectrum; (b) XPS Fe 2p spectrum; (c) XPS Zn 2p spectrum.

Fig. S12 XRD analysis of Au NPs.

Table S1 Catalytic HDO of palmitic acid in traditional meida.

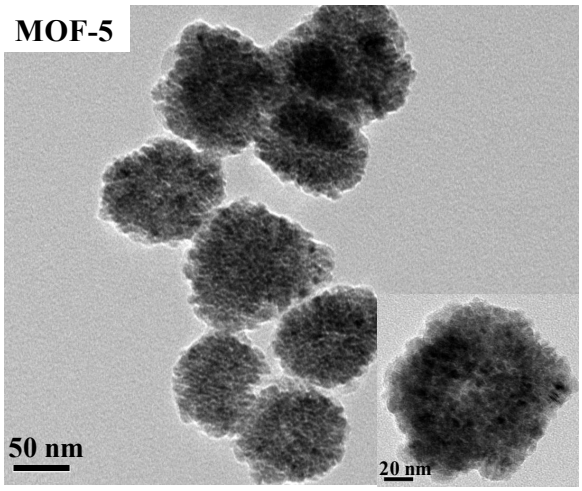

Fig. S1 TEM image of MOF-5.

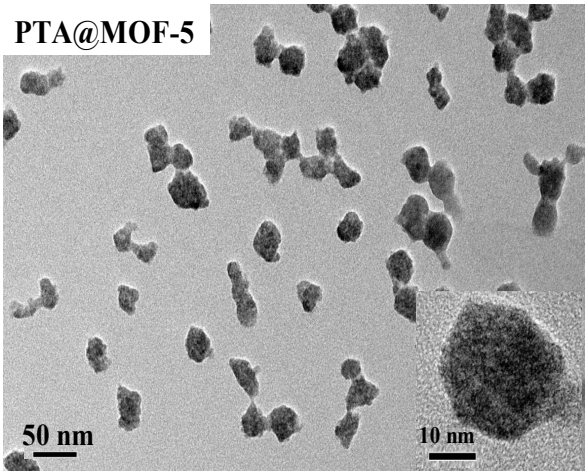

Fig. S2 TEM image of PTA@MOF-5.

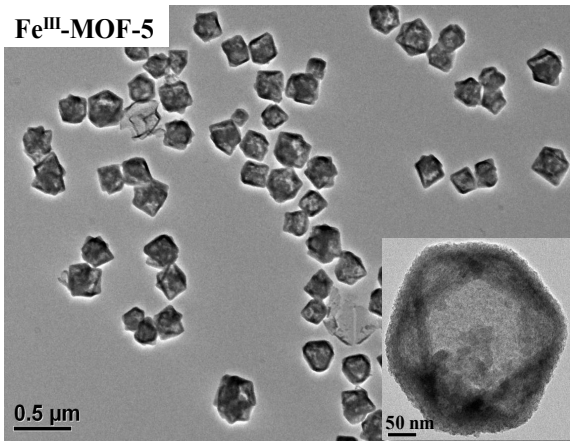

Fig. S3 TEM image of Fe^{III}-MOF-5.

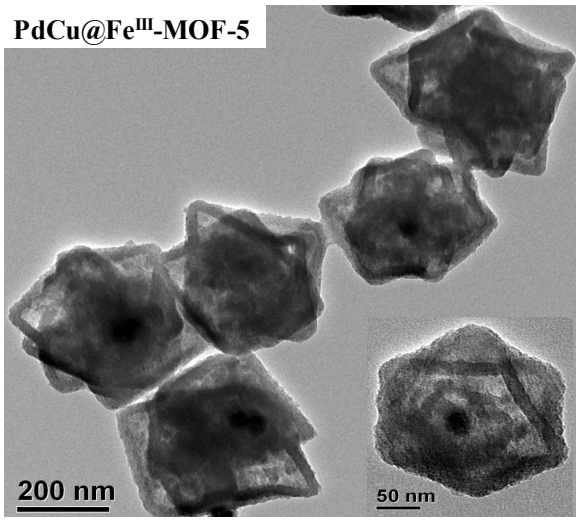

Fig. S4 TEM image of PdCu@Fe^{III}-MOF-5.

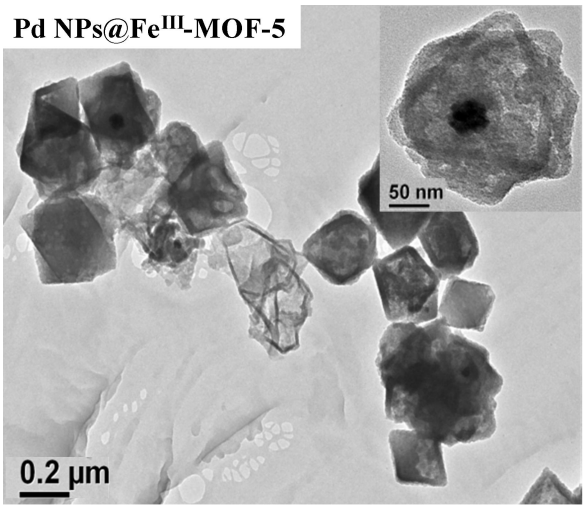

Fig. S5 TEM image of Pd NPs@Fe^{III}-MOF-5.

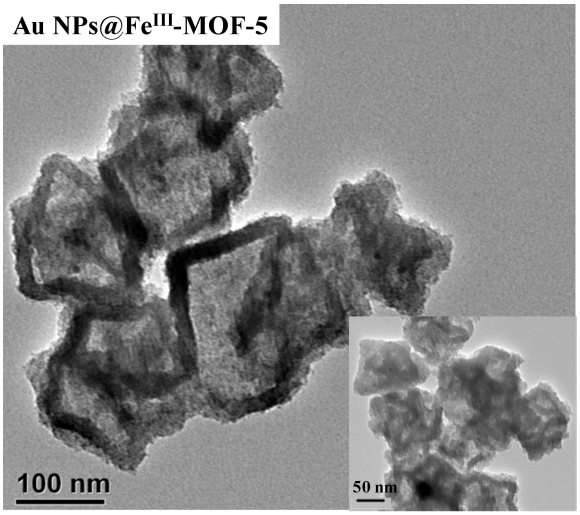

Fig. S6 TEM image of Au NPs@Fe^{III}-MOF-5.

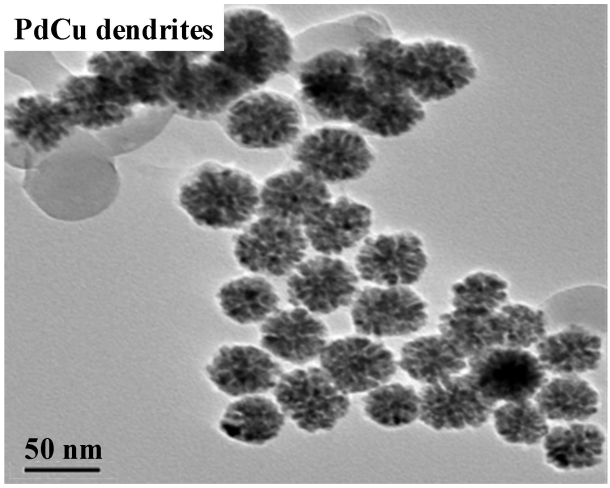

Fig. S7 TEM image of PdCu dendrites.

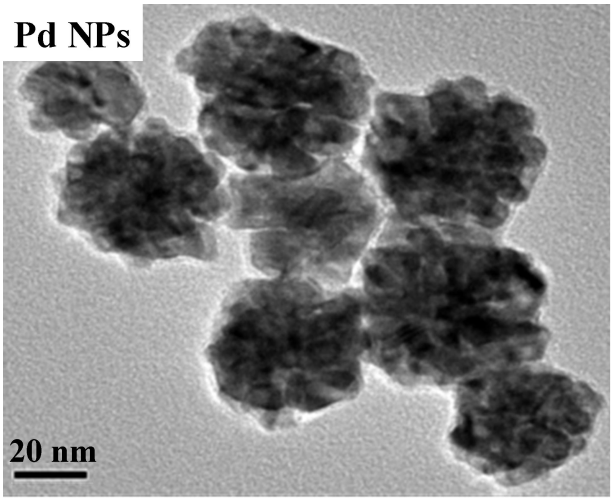

Fig. S8 TEM image of Pd NPs.

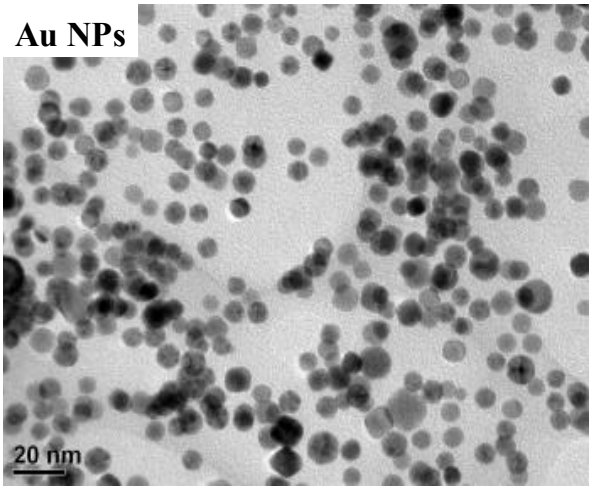

Fig. S9 TEM image of Au NPs.

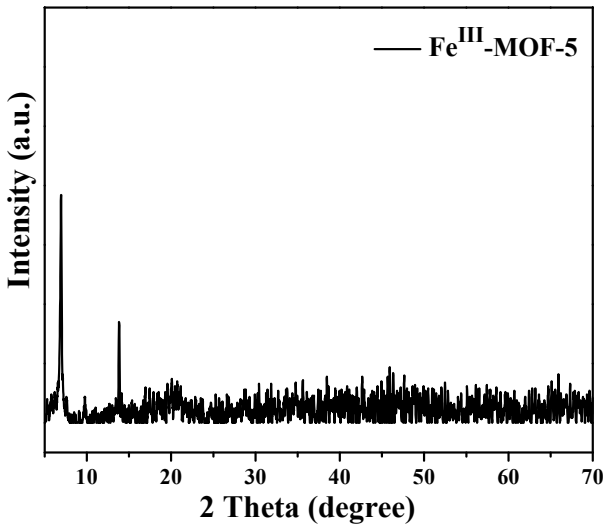

Fig. S10 XRD analysis of Fe^{III}-MOF-5.

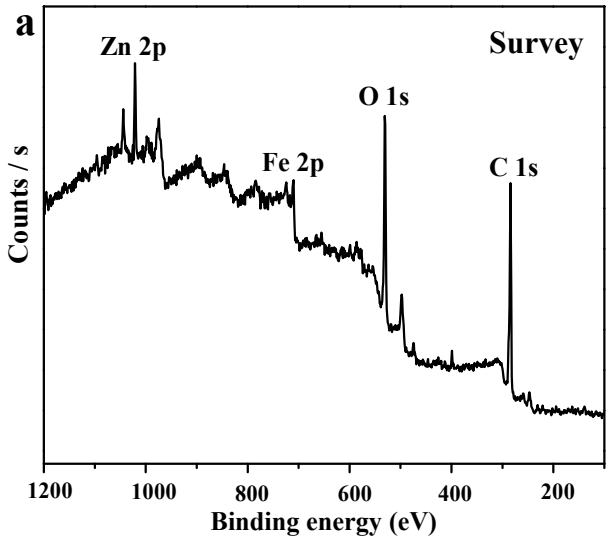

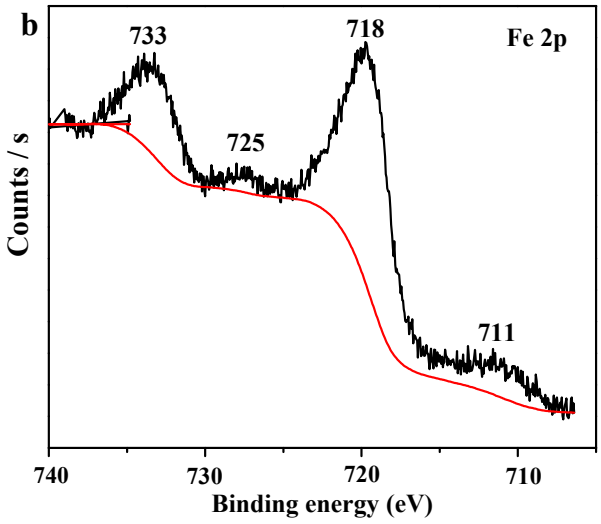

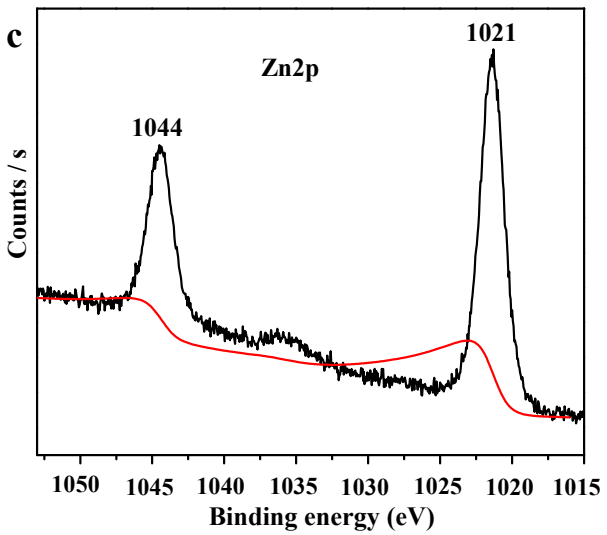

Fig. S11. XPS spectra of PTA@Fe^{III}-MOF-5 hollow octahedral nanostructures: (a) The survey spectrum; (b) XPS Fe 2p spectrum; (c) XPS Zn 2p spectrum.

As shown in Figure S11b, the Fe 2p peaks of Fe^{III}-MOF-5 hollow spheres at ~711 eV and ~725 eV are assigned to Fe 2p3/2 and Fe 2p1/2 for iron (III) oxide, and the additional satellite peaks at ~718 eV and ~733 eV are associated with Fe 2p3/2 and Fe 2p1/2, which exhibits similar spectra with those of Fe_2O_3. [3] The Zn 2p peaks at ~1021eV and ~1044 eV are assigned to Zn 2p3/2 and Zn 2p1/2 for zinc (II) oxide. [4]

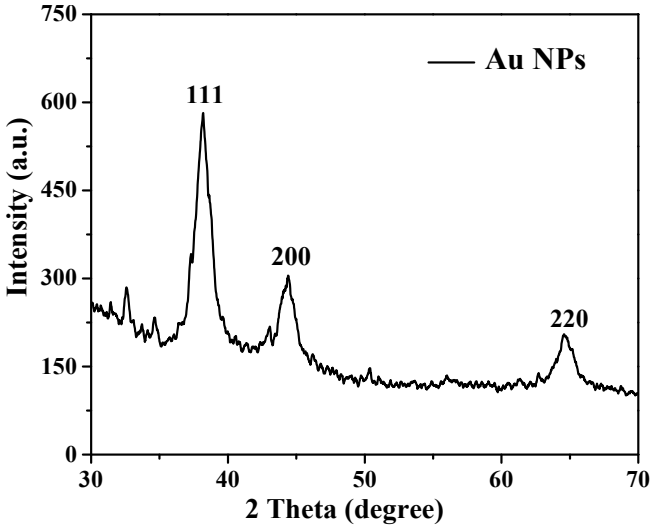

Fig. S12. XRD analysis of Au NPs.

As shown in Fig. S12, the XRD analysis of the as-synthesized Au NPs coincides

with the literatures [1, 2].

Table S1 Catalytic HDO of palmitic acid in traditional meida.

Catalyst	T / °C	t / h	P_{H2} / MPa	Conv. / %	Product distribution / %			
5 % MoO_2/CNTs [5]	220	4	4	100	Pentadecane / 7.60		Hexadecane / 92.20	
1.5 % Co-5 % MoO_2/CNTs [6]	180	4	4	100	Pentadecane / 5.20		Hexadecane / 89.30	
5 % Ni/CNTs [7]	240	4	2	97.25	Pentadecane / 89.64			
Mo/HZ-R [8]	260	4	4	100	n-C_{15} / 23.6	multi-iso-C_{16} / 15.6	mono- iso-C_{16} / 44.1	n-C_{16} / 15.8

References

1 Z. Zhang, Y. Chen, X. Xu, J. Zhang, G. Xiang, W. He and X. Wang, *Angew. Chem. Int. Ed.*, 2014, **53**, 429-433.

2 B. Xu, Z. Zhang and X. Wang, *Nanoscale*, 2013, **5**, 4495-4505.

3 Y. Yang, H. X. Ma, J. Zhuang and X. Wang, Inorg. Chem. 2011, 50, 10141-10151.

4 L. Wang, D. Zhao, S.-L. Zhong and A.-W. Xu, *CrystEngComm*, 2012, **14**, 6875-6880.

5 R. Ding, Y. Wu, Y. Chen, J. Liang, J. Liu and M. Yang, *Chem. Eng. Sci.*, 2015, **135**, 517-525.

6 R. Ding, Y. Wu, Y. Chen, H. Chen, J. Wang, Y. Shi and M. Yang, *Catal. Sci. Technol.*, 2016, **6**, 2065-2076.

7 Y. Duan, R. Ding, Y. Shi, X. Fang, H. Hu, M. Yang and Y. Wu, *Catal.*, 2017, **7**, 8

8 Y. Shi, Y. Cao, Y. Duan, H. Chen, Y. Chen, M. Yang and Y. Wu, *Green Chem.*, 2016, **18**, 4633-4648.